Experimental Section

Determination of NH₃: We adopt Nessler's reagent method to quantify the concentration of produced NH_3. The electrolytes after 2-h electrolysis were diluted 50 times due to the large concentration of produced NH_3. In detail, 0.1 mL sodium potassium tartrate solution and 0.1 mL Nessler's reagent was added to 5 mL of the diluted electrolyte. After shaking and standing for 20 minutes, the absorbance was measured at a wavelength of 420 nm. The concentration absorbance curve was calibrated by a serious of standard NH_4Cl solutions with different concentration. The fitting curve (y = 0.17739x − 0.00322, R^2 = 0.9996) shows good linear relation of absorbance value with NH_3 concentration.

Determination of NO_2^- : Griess method was adopt to quantify the concentration of NO_2^-. The electrolytes were diluted 50 times. In brief, 4-aminobenzenesulfonamide (20.0 g), H_3PO_4 (50 mL), N-(1-naphthyl)-ethylenediamine dihydrochloride (1.0 g), and deionized water (450 mL) was mixed as a color reagent. Then, 0.1 mL color agent was added to 5 mL of the diluted electrolyte. The absorbance was performed at a wavelength of 540 nm after the mixture stand 15 min in dark. The fitting curve (y =2.99322x − 0.0000420 R^2 = 0.9999) shows good linear relation of absorbance value with NO_2^- concentration.

Determination of NO_3^- : The electrolytes were diluted to the detection range. In brief,

0.1 mL 1 M HCl and 0.01 mL 0.8 wt % sulfamic acid solution were added to 5 mL of the diluted electrolyte. After shaking and standing for 15 minutes, the absorbance was measured at wavelengths of 220 nm and 275 nm. The final absorbance was calculated by the following equation: Abs = A_{220nm} - $2A_{275nm}$. The calibration curve was plotted by the concentration of ammonia standard solution versus the corresponding absorbance (y = 0.25197x + 0.00125 R^2 = 0.9998).

Determination of FE, NH_3 yield:
 The ammonia generation rate was calculated as the following equation:

$$r = \frac{C_{NH_3} \times V}{m_{cat.} \times t}$$

The FE of ammonia was calculated as the following equation:

$$FE_{NH_3} = \frac{C_{NH_3} \times V \times 8 \times F}{M_{NH_3} \times Q} \times 100\%$$

Where n represent the number of electrons transferred for NO_3RR (the reduction of NO_3^- to NH_3 consumes 8 electrons), F is the Faraday constant (96485 C mol^{-1}), C is the concentration of produced NH_3 calculated by fitting curves, V is the volume of cathodic reaction electrolyte (125 mL), M is the relative molecular mass of NH_3, Q is the total quantity of applied electricity, t is the reduction time (2 h), and m is the mass of catalyst (mg).

In situ Raman measurement: In situ Raman spectroscopy was performed on a Renishaw inVia Qontor Raman microscope system with a homemade three-electrode H-type in situ cell. The wavelength of the excitation source of the laser is 532 nm (10%). A 50 × long focal length distance objective (Leica) was used for focus. The graphite rod and Ag/AgCl electrode (saturated KCl solution) as the counter and reference electrodes, respectively. The spectrum was collected after 5 min of stable operation for each potential.

^{15}N isotope-labeling experiment: An isotope-labeling experiment with using 0.1M NaOH/0.1 M Na^{15}NO$_3$ as the electrolyte was carried out to clarify the source of NH_3. After electrolysis, the pH of the electrolyte was adjusted to 3 using 5 M H_2SO_4. Then, 0.5 mL of the above solution was taken out, followed by the addition of 50 μL of deuterium oxide for further quantification by 1H NMR (600 MHz). The standard calibration curve was also established using ^{15}NH$_4$Cl aqueous solutions with known concentrations (25, 50, 75, 100, 150 ppm).
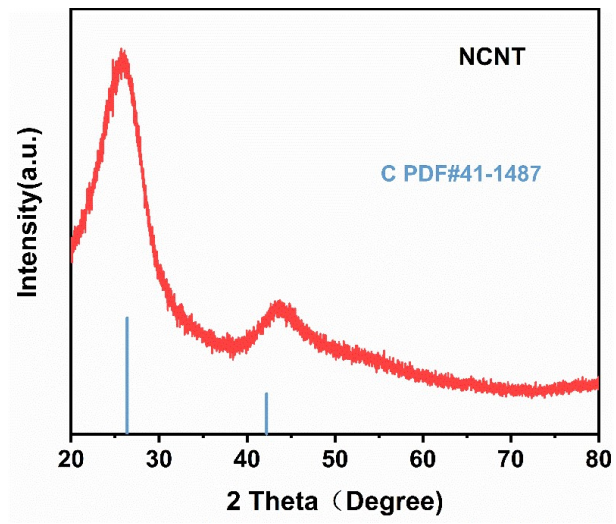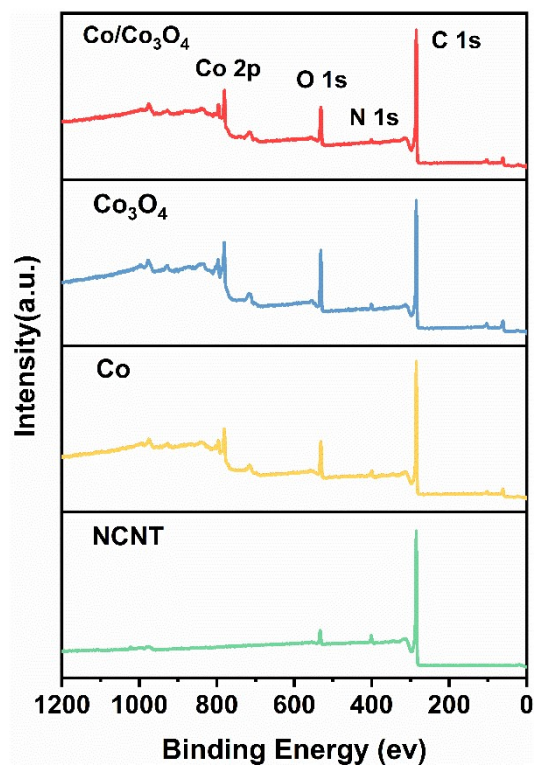
Figure S1. XRD images of NCNT.

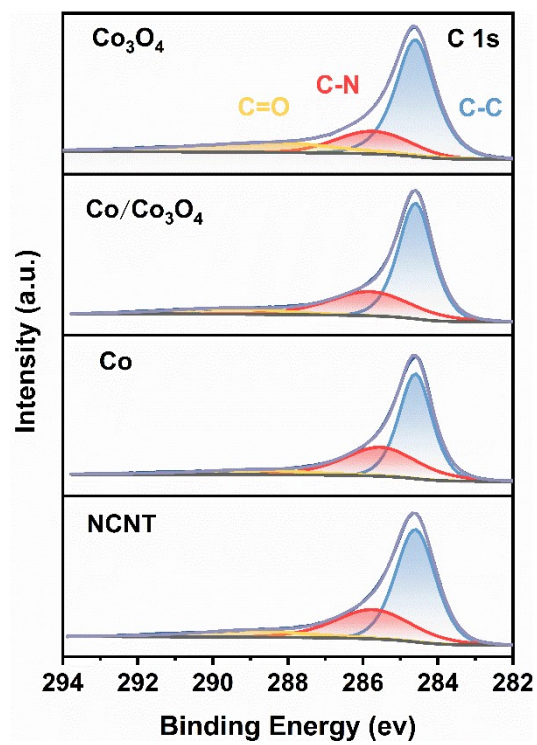**Figure S2.** XPS survey spectrum of Co/Co$_3$O$_4$@NCNT, Co$_3$O$_4$@NCNT, Co@NCNT, NCNT.

Figure S3. C 1s XPS spectra of Co/Co$_3$O$_4$@NCNT, Co$_3$O$_4$@NCNT, Co@NCNT, NCNT.
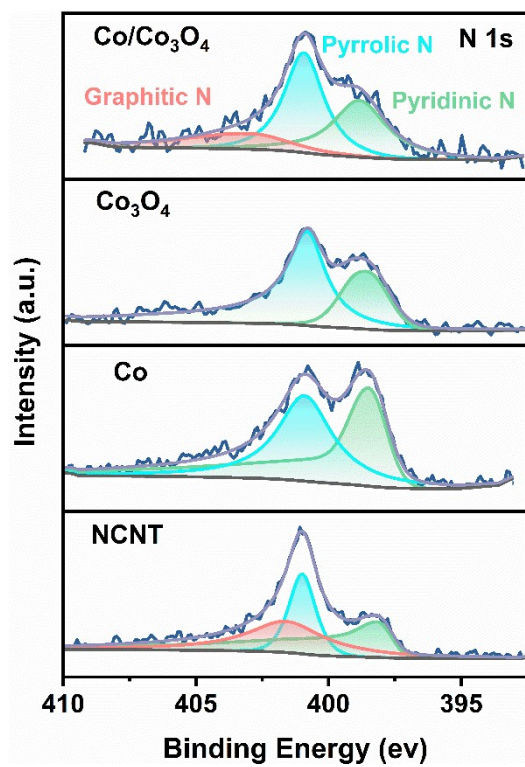
Figure S4. N 1s XPS spectra of Co/Co$_3$O$_4$@NCNT, Co$_3$O$_4$@NCNT, Co@NCNT, NCNT.
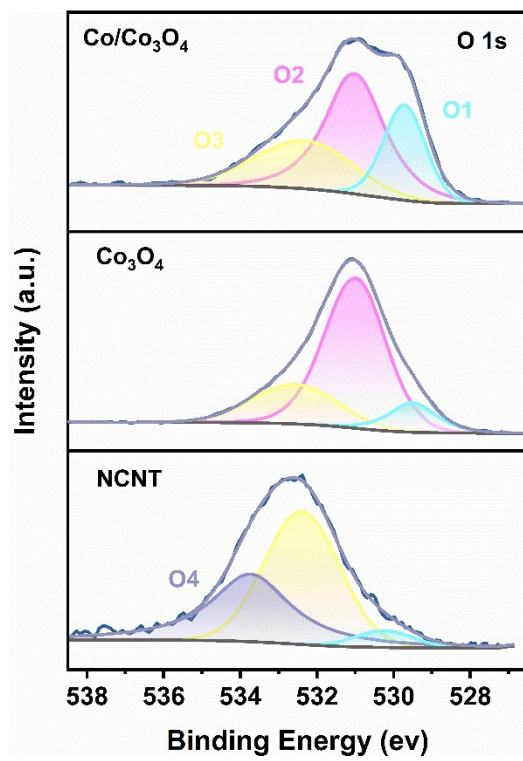
Figure S5. O 1s XPS spectra of Co/Co$_3$O$_4$@NCNT, Co$_3$O$_4$@NCNT, NCNT.
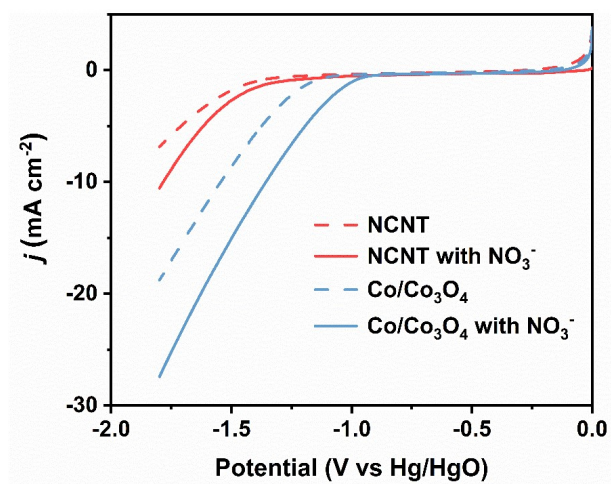
Figure S6. LSV curves of NCNT in 0.1 M NaOH with and without 0.1M NO_3^-.
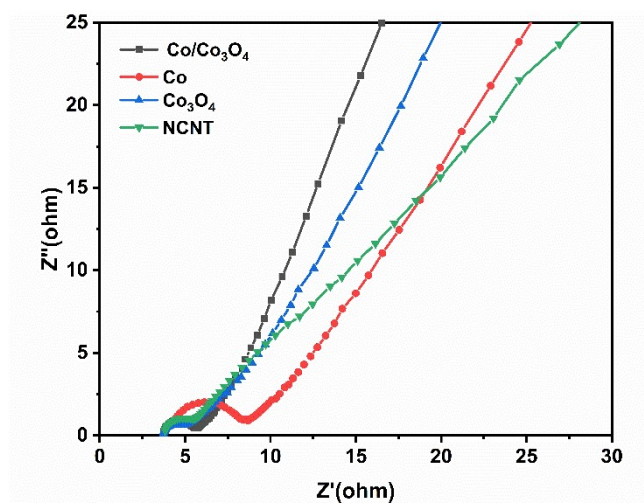
Figure S7. EIS curves of Co@NCNT, Co$_3$O$_4$@NCNT, Co/Co$_3$O$_4$@NCNT and NCNT at 0.1 V/s in a 0.1 M NaOH solution.
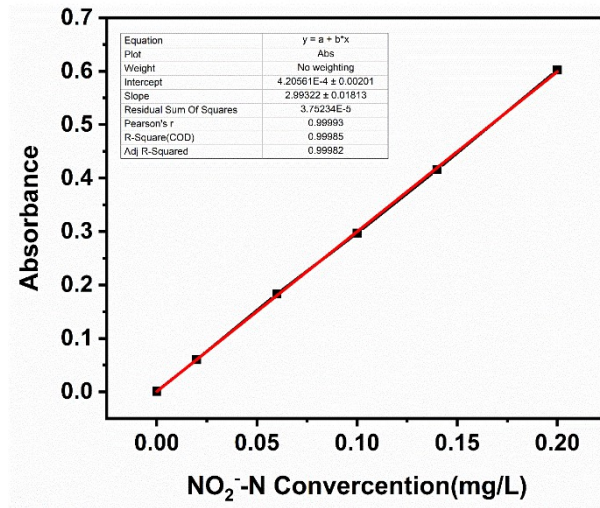
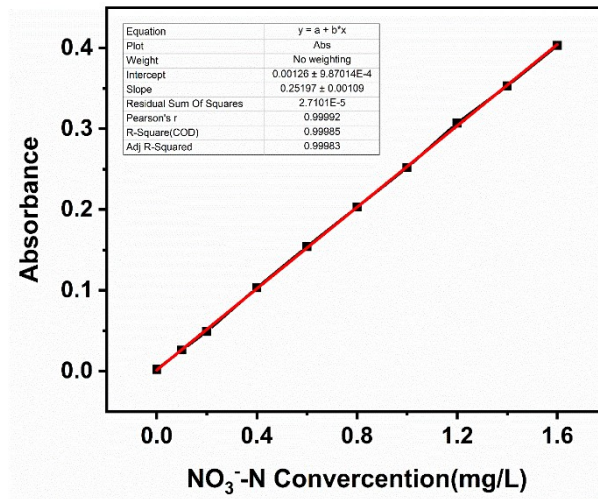**Figure S8.** The calibration curve used for calculation of NO_2^- concentration.

Figure S9. The calibration curve used for calculation of NO_3^- concentration.

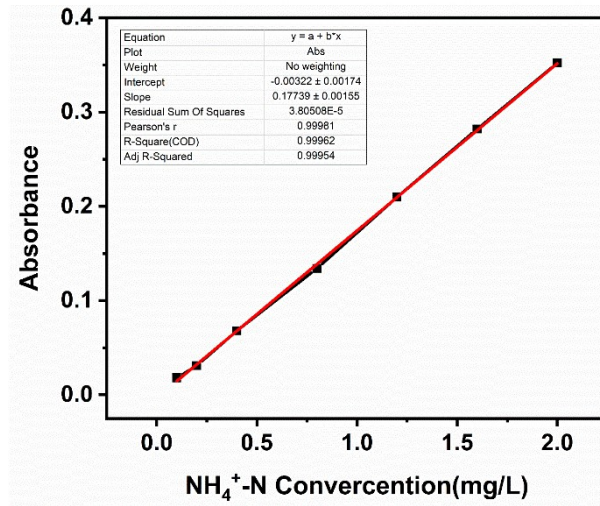| Equation	y = a + b*x
Plot	Abs
Weight	No weighting
Intercept	-0.00322 ± 0.00174
Slope	0.17739 ± 0.00155
Residual Sum Of Squares	3.80508E-5
Pearson's r	0.99981
R-Square(COD)	0.99962
Adj R-Squared	0.99954

Figure S10. The calibration curve used for calculation of NH_4^+ concentration.
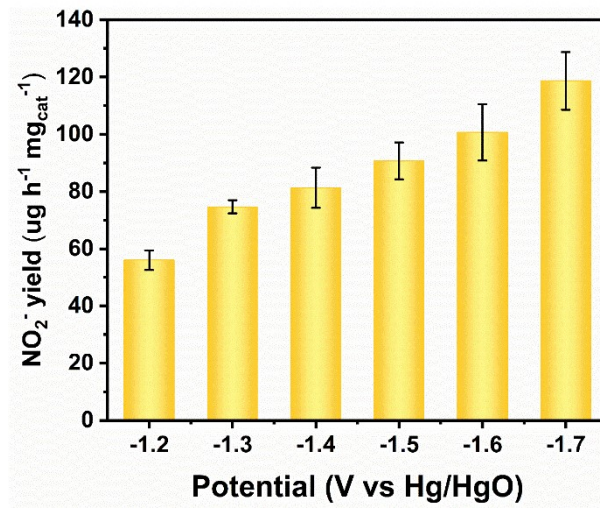
Figure S11. NO_2^- yields of $Co/Co_3O_4@NCNT$ at each given potential.

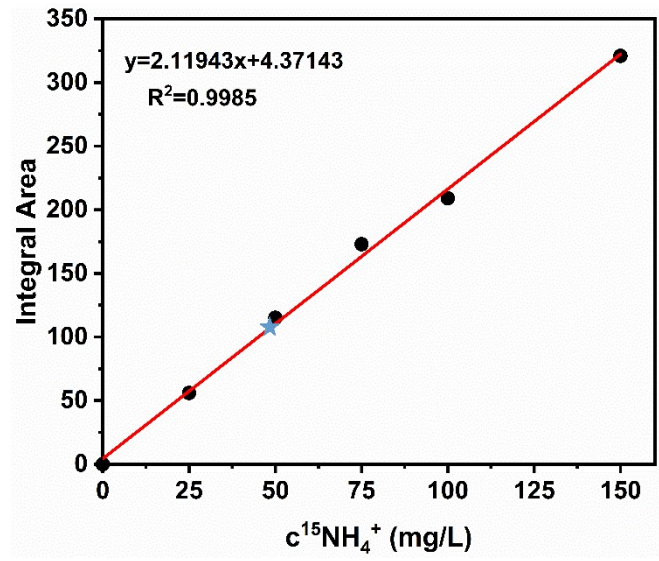**Figure S12.** Standard calibration curve of $^{15}NH_4^+$.
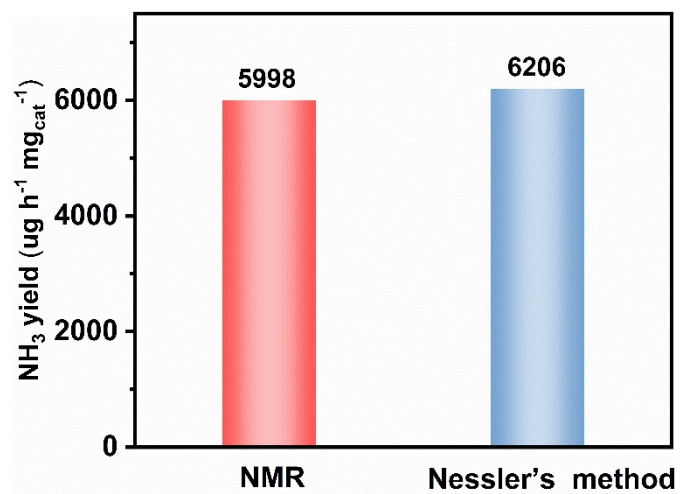
Figure S13. Produced ammonia yield determined by ^{1}H NMR and Nessler's method, respectively.
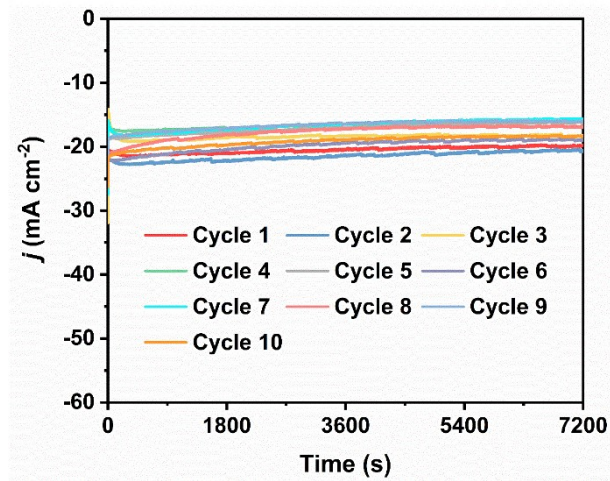
Figure S14. Chronoamperometry curves of Co/Co$_3$O$_4$@NCNT for generated NH$_3$ during recycling tests at −1.5 V vs. Hg/HgO in 0.1 M NaOH with additional 0.1 M NaNO$_3$.

Figure S15. (a-d) HRTEM images of Co/Co$_3$O$_4$@NCNT after 10 cycles.

Figure S16. (a) XRD pattern (b) XPS survey spectrum (c) Co 2p spectrum and (d) C 1s XPS spectra of Co/Co$_3$O$_4$@NCNT after 10 cycles.

Table S1. Comparison of the catalytic performances of Co/Co_3O_4@NCNT with the other reported

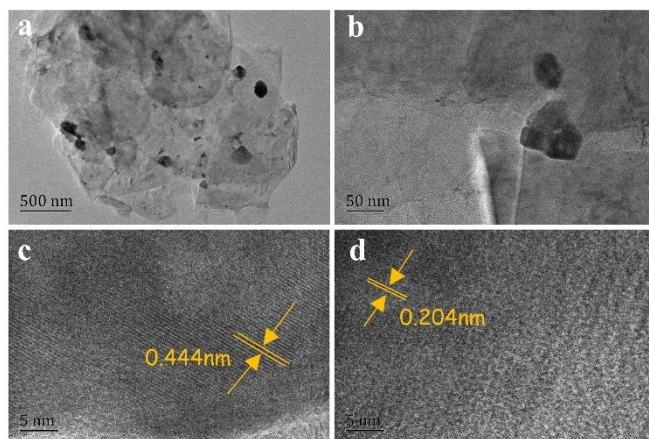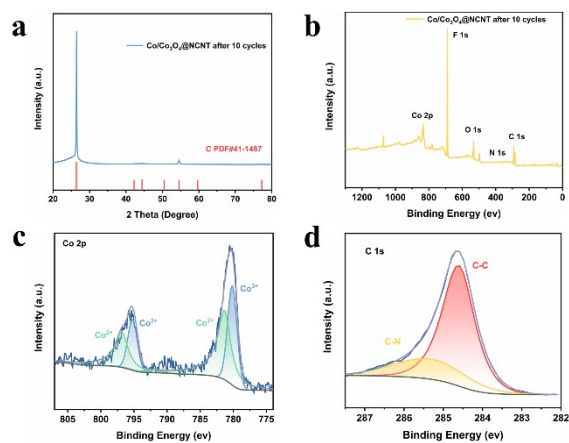NO_3^-RR electrocatalysts

Catalyst	Electrolyte	FE (100%)	NH_3 yield	Ref.
Co/Co_3O_4 @NCNT	0.1 M NaOH （0.1 M NO_3^-）	56%	6069 ug h^{-1} mg_{cat}^{-1}	This work
$ZnCo_2O_4$	0.1 M KOH （0.1 M NO_3^-）	75%	2100 ug h^{-1} mg_{cat}^{-1}	1
Cu_3P NA/CF	0.1 M PBS （0.1 M NO_3^-）	62.90%	847.96 ug h^{-1} mg_{cat}^{-1}	2
CoS_2 @TiO_2/TP	0.1 M NaOH （0.1 M NO_3^-）	85.14%	5790.87ug h^{-1} mg_{cat}^{-1}	3
FeS_2/RGO	0.5 M Na_2SO_4 （0.1 M NO_3^-）	83.70%	4640 ug h^{-1} mg_{cat}^{-1}	4
Cu−Pd/C	0.1 M KOH （10 mM NO_3^-）	62.30%	220 ug h^{-1} mg_{cat}^{-1}	5
Pd NDs/ZrMOF	0.1 M Na_2SO_4 （500ppmNO_3^-）	58.10%	4880 ug h^{-1} mg_{cat}^{-1}	6
Co_3O_4@NiO	0.5 M Na_2SO_4 (2.36 mM NO_3^-)	55%	….	7
Cu_2O (100)	0.1 M Na_2SO_4 （50ppm NO_3^-）	82.30%	743 ug h^{-1} mg_{cat}^{-1}	8
10Cu/TiO_{2-x}	0.5M Na_2SO_4 (200ppm NO_3^-)	81.34%	1943.1 ug h^{-1} mg_{cat}^{-1}	9
RM	1 M PBS （1 M NO_3^-）	92.80%	2720 ug h^{-1} cm^{-2}	10
FeOOH/CP	0.1 M PBS （0.1 M NO_3^-）	92%	2419 ug h^{-1} cm^{-2}	11
MnO_{2-x}	0.5 M Na_2SO_4 （0.1 M NO_3^-）	92%	3340 ug h^{-1} cm^{-2}	12
In-S-G	0.1 M NaOH （0.1 M NO_3^-）	75%	1271.94 ug h^{-1} cm^{-2}	13

References

1   P. Huang, T. Fan, X. Ma, J. Zhang, Y. Zhang, Z. Chen and X. Yi, 3D flower-like zinc cobaltite for electrocatalytic reduction of nitrate to ammonia under ambient conditions, *ChemSusChem*, 2022, **15**, e202102049.

2   J. Liang, B. Deng, Q. Liu, G. Wen, Q. Liu, T. Li, Y. Luo, A. A. Alshehri, K. A. Alzahrani, D. Ma and X. Sun, High-efficiency electrochemical nitrite reduction to ammonium using a Cu_3P nanowire array under ambient conditions, *Green Chemistry*, 2021, **23**, 5487-5493.

3   X.-E. Zhao, Z. Li, S. Gao, X. Sun and S. Zhu, $CoS_2@TiO_2$ nanoarray: a heterostructured electrocatalyst for high-efficiency nitrate reduction to ammonia, *Chemical Communications*, 2022, **58**, 12995-12998.

4   N. Zhang, G. Zhang, Y. Tian, Y. Tang and K. Chu, FeS_2 nanoparticles on reduced graphene oxide: an efficient electrocatalyst for nitrate electroreduction to ammonia, *Dalton Transactions*, 2022, **51**, 16805-16810.

5   Z. Wang, C. Sun, X. Bai, Z. Wang, X. Yu, X. Tong, Z. Wang, H. Zhang, H. Pang, L. Zhou, W. Wu, Y. Liang, A. Khosla and Z. Zhao, Facile synthesis of carbon nanobelts decorated with Cu and Pd for nitrate electroreduction to ammonia, *ACS Applied Materials & Interfaces*, 2022, **14**, 30969-30978.

6   M. Jiang, J. Su, X. Song, P. Zhang, M. Zhu, L. Qin, Z. Tie, J.-L. Zuo and Z. Jin, Interfacial reduction nucleation of noble metal nanodots on redox-active metal–organic frameworks for high-efficiency electrocatalytic conversion of nitrate to ammonia, *Nano Letters*, 2022, **22**, 2529-2537.

7   Y. Wang, C. Liu, B. Zhang and Y. Yu, Self-template synthesis of hierarchically structured $Co_3O_4@NiO$ bifunctional electrodes for selective nitrate reduction and tetrahydroisoquinolines semi-dehydrogenation, *Science China Materials*, 2020, **63**, 2530-2538.

8   J. Qin, L. Chen, K. Wu, X. Wang, Q. Zhao, L. Li, B. Liu and Z. Ye, Electrochemical synthesis of ammonium from nitrates via surface engineering in $Cu_2O(100)$ facets, *ACS Applied Energy Materials*, 2022, **5**, 71-76.

9   X. Zhang, C. Wang, Y. Guo, B. Zhang, Y. Wang and Y. Yu, Cu clusters/TiO_{2-x} with abundant oxygen vacancies for enhanced electrocatalytic nitrate reduction to ammonia, *Journal of Materials Chemistry A*, 2022, **10**, 6448-6453.

10   Y.-T. Xu, K.-C. Ren, Z.-M. Tao, D. K. Sam, E. Feng, X. Wang, G. Zhang, J. Wu and Y. Cao, A new catalyst based on disposed red mud for the efficient electrochemical reduction of nitrate-to-ammonia, *Green Chemistry*, 2023, **25**, 589-595.

11   Q. Liu, Q. Liu, L. Xie, Y. Ji, T. Li, B. Zhang, N. Li, B. Tang, Y. Liu, S. Gao, Y. Luo, L. Yu, Q. Kong and X. Sun, High-performance electrochemical nitrate

reduction to ammonia under ambient conditions using a FeOOH nanorod catalyst, *ACS Applied Materials & Interfaces*, 2022, **14**, 17312-17318.

12   G. Wang, P. Shen, Y. Luo, X. Li, X. Li and K. Chu, A vacancy engineered MnO$_{2-x}$ electrocatalyst promotes nitrate electroreduction to ammonia, *Dalton Transactions*, 2022, **51**, 9206-9212.

13   F. Lei, W. Xu, J. Yu, K. Li, J. Xie, P. Hao, G. Cui and B. Tang, Electrochemical synthesis of ammonia by nitrate reduction on indium incorporated in sulfur doped graphene, *Chemical Engineering Journal*, 2021, **426**, 131317.